

## Effects of Mutations of Aspartic Acid 63 on the Metal-Binding Properties of the Recombinant N-Lobe of Human Serum Transferrin<sup>†</sup>

Qing-Yu He,<sup>\*,‡</sup> Anne B. Mason,<sup>‡</sup> Robert C. Woodworth,<sup>‡</sup> Beatrice M. Tam,<sup>§</sup> Toby Wadsworth,<sup>§</sup> and Ross T. A. MacGillivray<sup>§</sup>

Department of Biochemistry, College of Medicine, University of Vermont, Burlington, Vermont 05405, and Department of Biochemistry and Molecular Biology, University of British Columbia, Vancouver, BC V6T 1Z3, Canada

Received December 10, 1996; Revised Manuscript Received February 24, 1997<sup>®</sup>

**ABSTRACT:** Mutations of the aspartic acid residue at position 63 of the N-lobe of human serum transferrin substantially alter the metal ion- and anion-binding properties of the protein. Substitution of serine, asparagine, glutamic acid, or alanine results in the loss of a key component of the interface in the interdomain cleft and the metal-binding ligand, aspartic acid, leading in all cases to an increased preference for NTA rather than carbonate as the “synergistic” anion relative to the wild-type protein. Excess bicarbonate is required to eliminate the NTA and obtain the “correct” visible spectrum. Carbonate replaces NTA *via* an intermediate. Blue shifts for the characteristic absorption band of each mutant show a range of effects on the Fe–O (Tyr) interaction. Titration with Co(III) yielded the molecular absorption coefficient for each mutant except D63A, where Co(III) appeared to oxidize the tyrosine residues and damage the ability of the mutant to bind metal. The chelator, Tiron, removes iron from hTF/2N with a simple saturation kinetic mode with respect to the ligand concentration. Chloride inhibits the release in an interesting manner: the effect is initially sharp and then levels off with a minimum  $k_{\text{obs}}$  at  $[\text{KCl}] = 0.5 \text{ M}$ . However, the reaction of the D63 mutants with Tiron results in the formation of the ternary complexes Fe–hTF/2N–Tiron. Significant red shifts for the characteristic absorption bands of these complexes suggest a different ligation of Tiron in the mutants from that in wild-type hTF/2N.

Human serum transferrin is an 80 kDa glycoprotein comprising two homologous lobes, each with the ability to bind reversibly a single ferric ion and a synergistic anion (carbonate). The protein plays an essential role in the sequestration of iron in the blood plasma, delivery of this iron to cells requiring iron, and buffering of free iron to such a low concentration that potential pathogens are deprived of the iron necessary for their growth (Griffiths, 1987; Harris & Aisen, 1989; Chasteen & Woodworth, 1990). Structural studies of three homologous proteins, human lactoferrin, rabbit serum transferrin, and chicken ovotransferrin, have shown that each of the two lobes (joined by a short bridging peptide) comprises two domains (I and II) that define a deep cleft containing the ligands, which bind the ferric ion and the synergistic anion, carbonate (Baker, 1994). In all of the structures, the ferric ion in each binding site is coordinated to the side chains of two tyrosines, one histidine, an aspartic acid, and two oxygens from the carbonate (Anderson et al., 1987; Bailey et al., 1988; Kurokawa et al., 1995). Numerous studies have shown that the site can be occupied by many different metal ions (Pecoraro et al., 1981; Harris & Madsen, 1988; Harris, 1983, 1986, 1989; Zak & Aisen, 1988; Abdollahi et al., 1996). Under suitable experimental conditions, other small carboxylates with a second electron-donor

group may also bind to the iron center at the binding sites of carbonate (Schlabach & Bates, 1975; Baker, 1994). These features have been employed to help characterize the physical and chemical properties of the protein. Biophysical studies indicate that significant conformational changes accompany metal binding (Rosseneu-Motreff et al., 1971; Kilar & Simon, 1985; Grossmann et al., 1992, 1993). These changes appear to be critical for receptor recognition, binding, and transport of iron into cells. Crystallographic studies of lactoferrin detail the conformational changes at the molecular level. Superposition of the apo- and iron-loaded N-lobe reveals a 54° domain rotation about a central point on the two antiparallel interdomain strands (Anderson et al., 1990). Closure of the protein apparently involves two hinges which produce a “see-saw” motion. In the open form a small interface (involving 13 residues) is buried, and a large interface (involving twice as many residues) is solvent accessible. In the closed form the situation is reversed. Apparently, there is very little difference in energy between the two forms, which means that, in the absence of bound metal ion, there should be an equilibrium between the open and closed conformations (Gerstein et al., 1993). This lends support to the idea that the closed C-lobe observed in apolactoferrin is a crystallization artifact. In fact, another structure of apolactoferrin has been solved in which the cleft is open (Baker, 1994).

<sup>†</sup>This work was supported by USPHS Grant R01 DK 21739 (to R.C.W.) from the National Institute of Diabetes and Digestive and Kidney Diseases. Q.-Y.H. was supported by the Dean's Postdoctoral Fellowship from the College of Medicine at the University of Vermont.

\* Corresponding author. Telephone: (802) 656-0343. Fax: (802)-862-8229. E-mail: QHE@zoo.uvm.edu.

<sup>‡</sup> University of Vermont.

<sup>§</sup> University of British Columbia.

<sup>®</sup> Abstract published in *Advance ACS Abstracts*, April 15, 1997.

<sup>1</sup> Abbreviations: hTF, human serum transferrin; hTF/2N, recombinant N-lobe of human transferrin comprising residues 1–337 (mutants of hTF/2N are designated by the wild-type amino acid residue, the sequence number, and the amino acid to which the residue was mutated); BHK, baby hamster kidney cells; NTA, nitrilotriacetate; EDTA, ethylenediaminetetraacetate; Tiron, 4,5-dihydroxy-1,3-benzene-disulfonate.

Recombinant DNA technology allows one to study differences in spectroscopic and other properties of mutants in which single amino acids have been changed. This approach provides a unique opportunity to understand this complex system. The recombinant N-lobe of human serum transferrin (hTF/2N)<sup>1</sup> and a number of single point mutants, including D63S and D63C, have been expressed and purified in this laboratory; differences in their ability to bind iron have been reported (Woodworth et al., 1991; Lin et al., 1993). The aspartic acid at position 63 is the only ligand provided from domain I of the N-lobe. A crystal structure of the equivalent mutant (D60S) of the lactoferrin N-lobe has recently been published (Faber et al., 1996). In addition to binding iron, the aspartic acid in the N-lobe of lactoferrin provides important stabilizing interactions in the "closed" structure through a carboxylate oxygen atom which forms hydrogen bonds linking two helices in domains I and II. In the mutant, the substituted serine does not coordinate to iron directly; instead, a water molecule fills the iron coordination site and participates in interdomain hydrogen bonding. In the lactoferrin mutant the cleft is more closed than in the unmutated N-lobe. This result is in contrast to the low-angle X-ray studies of the D63S mutant of the human transferrin N-lobe in which the cleft is reported to be open (Grossmann et al., 1993).

In the present report, a family of mutants, D63S, D63E, D63N, and D63A, in which the Asp ligand was mutated to Ser, Glu, Asn, and Ala, respectively, have been produced, purified, and characterized. Along with the wild-type hTF/2N, these mutants were studied in order to compare differences in spectroscopy, metal-binding, and exchange and iron-release kinetics. The aim of the work is to show the effect of this change in the specific iron-binding residue, Asp 63, on the properties of the protein.

## MATERIALS AND METHODS

**Materials.** Chemicals were reagent grade. Stock solutions of HEPES, MES, and other buffers were prepared by dissolving the anhydrous salts in Milli-Q purified water and adjusting the pH to desired values with 1 M NaOH or HCl. A standard solution of cobalt (1000  $\mu\text{g/mL}$ , AAS standard solution, Specpure) was obtained from Alfa Aesar. Tiron came from Fisher Scientific Co. Centricon 10 microconcentrators were from Amicon.

**DNA Manipulations.** The construction of the D63S mutant of the N-lobe of human transferrin has been described previously (Woodworth et al., 1991). The mutants D63A, D63E, and D63N were constructed in the hTF/2N cDNA using PCR-based mutagenesis. An *Xba*I–*Bam*HI fragment of the human transferrin cDNA (Funk et al., 1990) was subcloned into the plasmid Bluescript SK; this DNA fragment contains part of the 5' untranslated region of transferrin mRNA followed by the coding region for residues –19 to 337 of transferrin. *In vitro* mutagenesis was performed utilizing Bluescript-specific flanking oligonucleotides and the following mutagenic oligonucleotides as primers:

D63A: 5'-GTGACACTGGCTGCAGGTTTG-3'  
D63E: 5'-TGACACTGGAAGCAGGTTTGG-3'  
D63N: 5'-TGTGACACTGAATGCAGGTTT-3'

In each case, the mutagenic nucleotide is underlined. Mutagenesis was carried out as described by Nelson and

Long (1989) using the following conditions: denaturation was at 94 °C for 15 s, annealing was at 50 °C for 30 s, and extension was at 72 °C for 30 s. Step I of the PCR mutagenesis procedure consisted of 30 cycles, step II consisted of two cycles, and step III consisted of 30 cycles.

The PCR products from each of the three mutagenesis reactions were digested with *Xba*I and *Bam*HI and ligated into the *Xba*I and *Bam*HI sites of Bluescript SK containing the hTF/2N cDNA. The nucleotide sequences of the *Xba*I–*Bam*HI inserts were then determined to confirm the introduction of the specific mutation and to ensure that no other mutations had been introduced during the PCR steps. The mutated hTF/2N cDNAs were then excised from the Bluescript vector by digestion with *Xba*I and *Hind*III, the ends were made blunt by treatment with the Klenow fragment of *Escherichia coli* DNA polymerase I in the presence of dNTPs, and the blunt-ended was fragment ligated into the *Sma*I site of the expression vector pNUT (Funk et al., 1990). The correct orientation of the hTF/2N cDNA in the pNUT vector was confirmed by restriction endonuclease mapping.

**Expression, Isolation, and Purification of Proteins.** The N-lobe of hTF and its D63 single point mutants were expressed into the medium of BHK cells containing the relevant cDNA in the pNUT vector and were purified as described previously (Woodworth et al., 1991; Mason et al., 1991). Removal of iron from the transferrin samples was accomplished by treatment of the proteins in Centricon 10 microconcentrators with 0.5 M sodium acetate, pH 4.9, containing 1 mM NTA and 1 mM EDTA, until no color was observed. The protein was then sequentially washed with 2 mL of 0.1 M KCl, 2 mL of 0.1 M sodium perchlorate, and 4  $\times$  2 mL of 0.1 M KCl. At this point the protein, still in the Centricon, was exhaustively exchanged into the buffer of choice (see below). Fe-saturated transferrin was prepared by adding a slight excess of Fe(NTA)<sub>2</sub> to a buffer solution (pH 7.4) containing the apoprotein and bicarbonate, letting it stand at room temperature for 1 h or overnight at 4 °C, and then exchanging the sample into the desired buffer (50 mM HEPES, pH 7.4).

**Spectra and Co(III) Titration.** UV–visible spectra were recorded on a Cary 219 spectrophotometer under the control of the computer program Olis-219s (On-line Instrument Systems, Inc., Bogart, GA). The appropriate buffer served as the reference for full-range spectra from 240 to 650 nm. Co(III) titrations to determine extinction coefficients,  $\epsilon$ , for each mutant were conducted as described previously with sodium bicarbonate/CO<sub>2</sub> buffer (He et al., 1996). Titration of wild-type hTF/2N was performed prior to titration of each mutant sample to standardize the procedure. The reported results are the average values derived from at least two titrations.

**Anion-Exchange Studies between NTA<sup>2-</sup> and Carbonate.** A spectrum showing the characteristic absorption band in the visible region for a normal ferric D63 mutant (carbonate complex, yellow,  $\sim$  40  $\mu\text{M}$ ) in 50 mM HEPES (pH 7.4) was recorded. After an equivalent of NTA<sup>2-</sup> was added to the solution, spectroscopic scans were made to generate a stable curve for the NTA<sup>2-</sup> complex of the mutant iron protein (pink). Then increasing amounts of bicarbonate (stock solution, 0.5 M) were added to the solution until the yellow color was recovered completely. During the titration, spectra were taken after each addition. About 4 min was required to reach equilibrium after each addition.

Table 1: Summary of Spectral Characteristics and Extinction Coefficients for Recombinant Wild Type (WT) and Mutants of hTF/2N

mutant	$\lambda_{\max}$ (nm) <sup>a</sup>	$\lambda_{\min}$ (nm) <sup>a</sup>	$A_{\max}/A_{\min}$	$A_{280}/A_{\max}$	$\lambda_{\text{Co(III)}}^{\text{max}}$ (nm) <sup>b</sup>	$\lambda_{\text{NTA}}^{\text{max}}$ (nm) <sup>c</sup>	$\lambda_{\text{Tiron}}^{\text{max}}$ (nm) <sup>d</sup>	$\epsilon_{280}$ (mM <sup>-1</sup> ·cm <sup>-1</sup> ) <sup>e</sup> , Co(III) titration
D63S	426	380	1.13 ± 0.01	22.8 ± 0.2	375	470	502	40.2 ± 0.3
D63E	450	396	1.19 ± 0.01	21.6 ± 0.1	395	471	534	31.6 ± 0.2
D63N	422	388	1.09 ± 0.02	21.4 ± 0.1	380	456	472	28.15 ± 0.01
D63A	414	402	1.02 ± 0.01	21.2 ± 0.2	366 <sup>b</sup>	468	483	
WT	472	410	1.37 ± 0.02	23.5 ± 0.1	407	470	470	38.5 ± 0.6 <sup>f</sup>

<sup>a</sup> 25 mM HEPES, pH 7.4, Fe-carbonate-hTF/2N ternary complexes. The small differences of these results for D63S and wild-type hTF/2N from the values reported previously (Woodworth et al., 1991) are accounted for by the different reference solutions used. In the present report, HEPES buffer or KCl solution rather than apoprotein served as references. <sup>b</sup> 10 mM NaHCO<sub>3</sub>, pH 8.5, Co-carbonate-hTF/2N ternary complexes;  $\lambda_{\text{Co(III)}}^{\text{max}}$  for D63A is unstable. <sup>c</sup> 50 mM HEPES, pH 7.4, Fe-NTA-hTF/2N ternary complexes. <sup>d</sup> 50 mM HEPES, pH 7.4, Fe-Tiron-hTF/2N ternary complexes. <sup>e</sup> 10 mM NaHCO<sub>3</sub>, pH 8.5, with 5% CO<sub>2</sub>. Values are means ± SD, calculated for the apoproteins. <sup>f</sup> From He et al. (1996).

**Kinetics of Iron Release.** Iron release reactions were performed in a quartz cuvette (3 mL, maintained at 25 ± 0.1 °C) and monitored by UV-visible spectroscopy using a Cary-219 spectrophotometer equipped with a thermostated cell. The computer program Olis-219s-Assay was used to run the time-based spectral measurements. Filtered iron-loaded transferrin (0.2 μm Acrodisc) was added into the sample cuvette containing the desired buffer (50 mM HEPES and 0 or 0.5 M KCl, pH 7.4). The final concentration of the protein was 40–45 μM. All assays were measured against a reference solution which contained the appropriate amount of buffer (50 mM HEPES, pH 7.4), KCl (0 or 0.5 M), and chelator (1–30 mM Tiron). The pair of matching cuvettes containing the sample and the reference was equilibrated in the thermostated cuvette chamber for 10–15 min before the measurement was started.

The time of mixing was recorded as 0 time. For iron release from wild-type hTF/2N by Tiron, the absorbance increase at 480 nm (Nguyen et al., 1993) was monitored and recorded every 0.5–5 min depending on the reaction rate until at least 3 half-lives had elapsed. Rate constants were obtained by fitting the absorbance *vs* time data to a single exponential function with the user-defined, nonlinear equations in the Axum program (MathSoft, 1996). For most of the calculations, the initial and final absorbance values ( $A_0$  and  $A_\infty$ ) were treated as adjustable parameters as long as their values stayed within experimentally reasonable boundaries. The reported values represent the average curve-fitting results from measurements made in triplicate.

## RESULTS AND DISCUSSION

**Absorption Spectra.** The D63S mutant was based on the naturally occurring mutation found in the C-terminal lobe of melanotransferrin (Rose et al., 1986). The other mutants are a logical extension of the D63S mutant. The glutamic acid mutant, D63E, was made to see whether the cleft could accommodate a side chain with one additional methylene carbon. The asparagine mutant, D63N, was made to determine whether both carboxyl oxygens are critical to tight metal binding, and the alanine mutant, D63A, was made to eliminate all H-bonding capability. Full scans from 240 to 650 nm gave entire UV-visible spectra for the mutants. Table 1 lists  $\lambda_{\max}$ ,  $\lambda_{\min}$  and  $A_{\max}/A_{\min}$ ,  $A_{280}/A_{\max}$  ratios, which were obtained from the spectra and can be regarded as some of the intrinsic spectral parameters for the mutants. The spectra in the visible region showing the  $\lambda_{\max}$  for each mutant protein are shown in Figure 1. The  $\lambda_{\max}$  expresses the energy level of the charge transfer between tyrosine ligands and the iron center (Gaber et al., 1974; Patch & Carrano, 1981; Faber

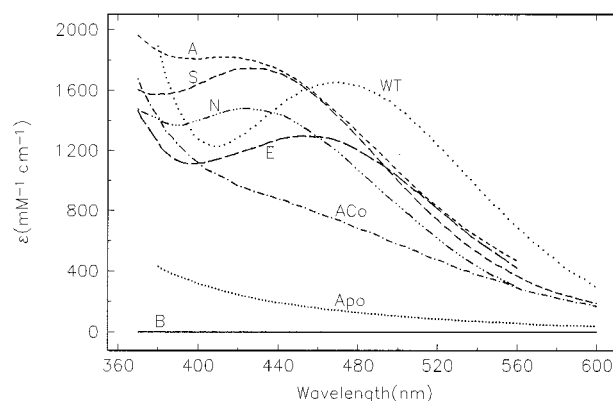


FIGURE 1: Visible spectra for the iron-saturated hTF/2N of transferrin. Concentrations were calculated with the  $\epsilon_{280}$  from Co(III) titration; for D63A, the  $\epsilon_{280}$  of WT was used in the calculation. Curves (A) D63A; (ACo) iron resaturation of D63S after Co(III) titration and removal of Co(III); (Apo) apo form of wild-type hTF/2N; (B) baseline; (E) D63E; (N) D63N; (S) D63S; (WT) wild-type hTF/2N.

et al., 1996). In all the mutants compared to wild-type hTF/2N, the  $\lambda_{\max}$ 's are blue shifted to considerably lower wavelengths ranging from 58 to 22 nm below the  $\lambda_{\max}$  for hTF/2N. In the D60S mutant of lactoferrin there was a 20 nm shift in  $\lambda_{\max}$ , 434 *vs* 454 nm for the wild-type N-lobe. The D63S maximum is shifted 46 nm relative to wild-type hTF/2N. If, as in the D60S mutant of lactoferrin, there is a water molecule bound to the ferric ion and linked to the serine residue with a hydrogen bond, this weaker ligation might allow a stronger Fe-O(Tyr) interaction (Faber et al., 1996). The differences in  $\lambda_{\max}$  for the D63 mutants might then be predicted to be due to variable effects from the substituted residues on the hydrogen bond to the coordinated water, which subtly change the Fe-O(Tyr) interaction. The D63E mutant has a  $\lambda_{\max}$  close to that of wild-type hTF/2N but showed a very facile iron release by EDTA, similar to D63S (He et al., unpublished results). A possible explanation is that Glu 63, as Asp 63 in the wild-type protein, is a ligand to the iron, but the cleft surrounding the binding site remains open to some degree, making the bound metal easily approached by chelates. Another possibility is that, like the situation in D60S mutant of lactoferrin, the Glu residue in D63E does not bind to the iron ion directly even though Glu differs only by a methylene group from Asp. In this case, a negative charge on Glu may help strengthen the coordination of water to iron *via* a hydrogen bond resulting in only a minor blue shift of  $\lambda_{\max}$ . In contrast,  $\lambda_{\max}$  for D63A has the largest decrease in wavelength; loss of all charge and of any electron-donor effect make it impossible for Ala to

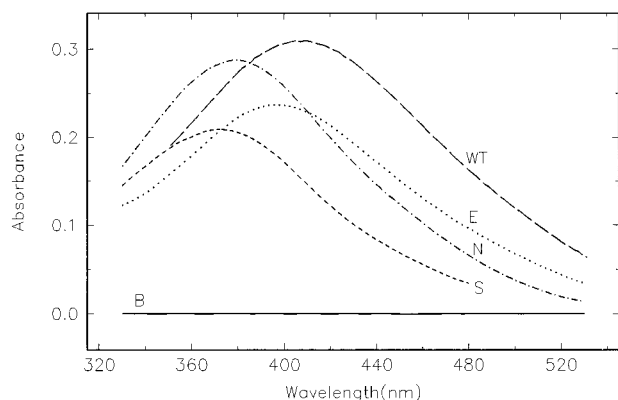


FIGURE 2: Visible absorbance bands for Co(III) transferrins. Concentrations are *ca.* 35  $\mu$ M based on  $\epsilon_{280}$  values from Co(III) titration. Curves (B) baseline; (E) D63E; (N) D63N; (S) D63S; (WT) wild-type hTF/2N.

participate in formation of a hydrogen bond. Both Ser and Asn, although lacking any charge, are still capable of forming a hydrogen bond with water. The question remains as to whether the cleft is open, closed, or in equilibrium between the two. Absence of the liganding aspartic acid may result in a failure to "lock in" the closed structure.

It must be pointed out that weakening an iron-binding ligand by means of mutation is not the only way to cause a blue shift of  $\lambda_{\max}$ , an indicator of the Fe—O(Tyr) interaction. Kurokawa et al. (1994) showed that the dissociation and reassociation of two proteolytically derived fragments of ovotransferrin caused a reversible blue shift. This indicates that intralobe peptide—peptide interactions can significantly affect the charge transfer of the Fe—O (Tyr) and subtly change the iron-binding ability of the protein.

**Co(III) Titration.** Another characteristic parameter, the extinction coefficient at 280 nm, of the mutant apoproteins was determined by the Co(III) titration procedure for all except the D63A mutant (He et al., 1996). The complexation between Co(III) and the mutants D63S, D63E, or D63N in sodium bicarbonate solution generated a stable, medium-intensity absorption band ( $\epsilon \sim 9000 \text{ M}^{-1} \text{ cm}^{-1}$ ,  $\lambda_{\max}^{\text{Co(III)}}$ , Table 1) in the visible region with the maxima at 375, 395, or 380 nm, respectively (Figure 2). Compared with the  $\lambda_{\max}$ 's for the iron-loaded proteins, these absorbance bands, together with that for wild-type hTF/2N, have a significant blue shift of 40–70 nm, suggesting that Co(III) has a stronger interaction with tyrosine and greater charge-transfer intensity than Fe(III) in the binding site of the proteins. Moreover, these  $\lambda_{\max}^{\text{Co(III)}}$  values have an order WT > D63E > D63S ~ D63N > D63A, similar to the order for the original iron forms, showing the extent of the interaction between the metal center and the tyrosine ligands. Titration curves with sharp break points were obtained for the Co(III) titrations of D63S, D63E, and D63N in 10 mM NaHCO<sub>3</sub>, pH 8.5. The resulting  $\epsilon_{280}$  values together with that for wild-type hTF/2N are given in Table 1. The differences in the extinction coefficients of the mutants is intrinsically interesting because, in theory, all should have the same  $\epsilon_{280}$  because there are the same number of Tyr, Trp, and Cys residues in each protein (Pace et al., 1995).

For D63A, Co(III) titration did not give the desired curves due to the fact that the absorbance maximum (366 nm initially) shifted with time, while the  $A_{280}$  decreased during the titration, even under O<sub>2</sub>-free conditions. An inference

from these results is that the Co(III) gradually oxidized the tyrosine residues upon coordination with the mutant. The  $\lambda_{\max}^{\text{Co(III)}}$  value for D63A is the lowest (Table 1); accordingly, the interaction between Co(III) and the tyrosines in D63A could have enough strength to result in tyrosine oxidation by Co(III). This idea of oxidation by Co(III) was supported by means of the visible spectrum for the Fe-resaturated D63A after Co(III) titration and removal (curve ACo in Figure 1), from which, compared with the original D63A spectrum (curve A in Figure 1), tyrosine oxidation by Co(III) irreversibly destroys the iron-binding ability of D63A. This dramatically different behavior between D63A and the other mutants implies that the Co(III) interaction in the binding site is different from that of Fe(III). Perhaps Glu, Ser, or Asn coordinates directly to Co(III) whereas Ala, without any coordination atom, is unable to bind to the Co(III). This loss of a ligand could strengthen the interaction between the Co(III) and the tyrosine ligands in D63A, allowing oxidation to take place, as occurs with native hTF (Ross et al., 1995) and ovotransferrin (Hsuan, 1987) in the reaction with periodate.

**Anion Exchange of NTA<sup>2-</sup> and CO<sub>3</sub><sup>2-</sup> in Transferrin.** All of the Asp 63 mutants migrated on the gel filtration column (0.1 M ammonium bicarbonate) as yellow-colored bands. Upon addition of NTA<sup>2-</sup>, however, the mutant protein solutions became pink. To test the equilibration and exchange reaction between the Fe transferrins, CO<sub>3</sub><sup>2-</sup>, and NTA<sup>2-</sup>, stepwise titrations with HCO<sub>3</sub><sup>-</sup> in a HEPES buffer solution (pH 7.4) were conducted for each mutant. A typical family of titration curves for D63S is displayed in Figure 3A. Curve a is a visible absorption spectrum for the Fe—D63S—CO<sub>3</sub> complex, obtained from iron loading in a 100 mM HCO<sub>3</sub><sup>-</sup> solution followed by removal of excess bicarbonate; the absorbance maximum is at 426 nm (yellow). When an equivalent of NTA<sup>2-</sup> was added to the solution, the color changed instantly to pink and the absorbance band shifted to curve b, with a maximum at 470 nm. With increasing amounts of HCO<sub>3</sub><sup>-</sup> added to the solution, this peak at 470 nm shifted as shown in curve e where the absorbance maximum is around 450 nm. Addition of more bicarbonate caused the absorbance at 426 nm to increase, thereby recovering the absorbance band for the CO<sub>3</sub><sup>2-</sup> complex (curves f  $\rightarrow$  g  $\rightarrow$  a). An interesting aspect is that, during the titration before curve e, when the absorbance at 470 nm decreased, the absorbance at 426 nm did not increase simultaneously, as might be anticipated. Instead, the 426 nm band was recovered gradually after curve e. This implies that there may be an intermediate state through which the protein passed in going from the NTA<sup>2-</sup> complex to the CO<sub>3</sub><sup>2-</sup> complex.

In an attempt to model the change, a group of simulated spectra for the exchange of NTA<sup>2-</sup> and CO<sub>3</sub><sup>2-</sup> in iron complexes of D63S, in the absence of an intermediate species, was created by computer (Figure 3B). These spectra showed that the absorption maximum shifted gradually with the different concentration ratios of the two components and that the spectral pattern is different from the actual conversion reaction shown in Figure 3A.

These observations support two important conclusions: (1) NTA<sup>2-</sup> has a higher affinity than CO<sub>3</sub><sup>2-</sup> for binding to the iron center in all the D63 mutants. An equivalent of NTA<sup>2-</sup> was able to replace CO<sub>3</sub><sup>2-</sup> instantly, but the reverse required

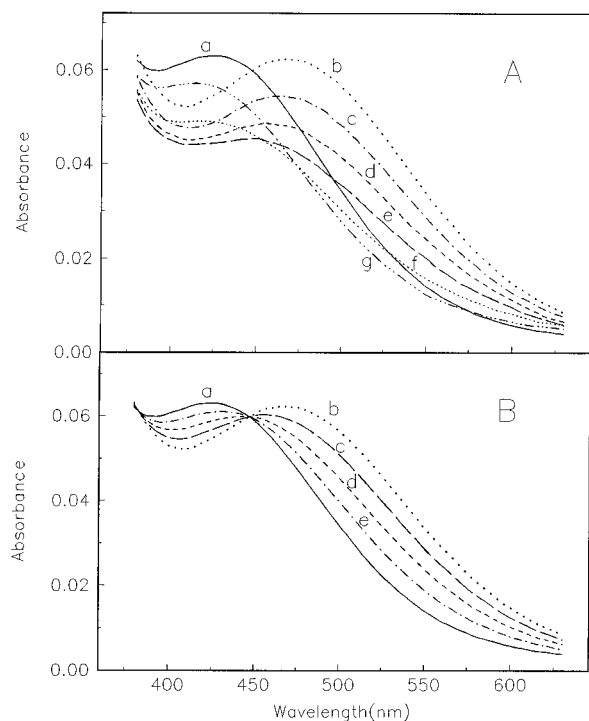


FIGURE 3: Comparison of visible spectra for the conversion between  $\text{CO}_3^{2-}$  and  $\text{NTA}^{2-}$  complexes of ferric D63S in HEPES (50 mM) solution, pH 7.4. (A) Actual spectra for the titration with bicarbonate: (a)  $\text{CO}_3^{2-}$  complex; (b)  $\text{NTA}^{2-}$  complex; (c–g) 15, 35, 65, 95, and 125 equivalents of bicarbonate, respectively, was added to (b). (B) Computer-simulated spectra for the transfer of the  $\text{CO}_3^{2-}$  and  $\text{NTA}^{2-}$  complexes of D63S in the absence of an intermediate species. The concentration ratios of  $[\text{CO}_3^{2-}]/[\text{NTA}^{2-}]$  are as follows: (a) 100:0; (b) 0:100; (c) 25:75; (d) 50:50; (e) 75:25.

a greater than 100-fold molar excess of  $\text{HCO}_3^-$ . In contrast, addition of bicarbonate to the wild-type hTF/2N complex of  $\text{NTA}^{2-}$  (under  $\text{CO}_2$ -free conditions) in 50 mM HEPES, pH 7.4, required only about an 8-fold molar excess of  $\text{HCO}_3^-$  to replace  $\text{NTA}^{2-}$  to form the natural  $\text{Fe-hTF/2N-CO}_3$  complex.<sup>2</sup> The absence of the Asp ligand in the D63 mutants appears to provide three iron coordination sites to the synergistic anion. For a single metal ion,  $\text{NTA}^{2-}$  is a potential tridentate ligand while  $\text{CO}_3^{2-}$  is only bidentate. Moreover, this loss of the Asp 63, the key linking component of the interdomain in the mutants (Faber et al., 1996), may lead to more inner flexibility for housing the bigger NTA anion. (2) An intermediate complex appears to be formed during the conversion from  $\text{Fe-D63S-NTA}$  to  $\text{Fe-D63S-CO}_3$ . This is possibly a quaternary complex involving  $\text{Fe}^{3+}$ , transferrin,  $\text{NTA}^{2-}$ , and  $\text{CO}_3^{2-}$ . A similar spectral change occurred during the exchange of  $\text{Fe}^{3+}$  between transferrin and acetohydroxamic acid, where a quaternary intermediate complex was also proposed (Coward et al., 1982).

As with D63S, the other mutants, D63E, D63N, and D63A, show a similar spectroscopic pattern during the exchange between  $\text{NTA}^{2-}$  and  $\text{CO}_3^{2-}$  complexes. Table 1 lists the wavelength of maximum absorbance ( $\lambda_{\text{max}}^{\text{NTA}}$ ) for the  $\text{NTA}^{2-}$  complexes, showing that between  $\lambda_{\text{max}}'$ s and  $\lambda_{\text{max}}^{\text{NTA}}$ s there

are large differences for the mutants and almost no change for wild-type hTF/2N. This means that, for the wild-type hTF/2N, such anion-exchange reactions are not easy to observe since they overlap almost completely with an absorbance maximum around 470 nm for both its  $\text{NTA}^{2-}$  and  $\text{CO}_3^{2-}$  complexes. The D63 mutants provide a unique opportunity for detecting the existence of an intermediate complex during the transfer. In conclusion, if we regard the carbonate complexes as representing the “natural” transferrin species, excess bicarbonate and adequate incubation time are required to obtain the iron–protein–carbonate complexes of the mutants.

**Kinetics of Iron Release by Tiron.** Tiron is a strong iron-sequestering agent. It effectively removes the ferric ion from native diferric transferrin with biphasic kinetic behavior, which can be followed simply with the absorption spectrum (Nguyen et al., 1993). A preliminary potentiometric pH titration showed that Tiron has two  $\text{pK}_a$  values at 5.0 and 9.7, respectively. In the presence of  $\text{Fe(III)}$ , the second deprotonation of Tiron occurs near pH 6.6 and is almost complete at pH 7.4. This means that a stable complex of Tiron and iron released from transferrin probably forms completely at pH 7.4. This pH has been used for kinetic studies. The  $\text{Fe(Tiron)}_3$  complex has a characteristic absorption maximum at 480 nm, close to the maximum at 472 nm for recombinant  $\text{Fe-hTF/2N(CO}_3)$ . Therefore, the absorption at 480 nm, which was monitored for the kinetic experiments, is the sum of the absorption from iron–protein and iron complexed with Tiron. Although Nguyen et al. used 460 nm to monitor iron release kinetics with Tiron, this also is a sum for the spectral absorptions of the two complexes (Nguyen et al., 1993). When an equivalent of  $\text{Fe-Tiron}$  (1:1) was added to the apo-hTF/2N without bicarbonate, allowed to stand at room temperature under  $\text{N}_2$  for 1 h and then washed thoroughly with HEPES buffer (pH 7.4), its visible spectrum showed a strong absorbance band at 470 nm. This probably is derived from the complex of  $\text{Fe-hTF/2N-Tiron}$ , where Tiron acts as a ‘synergistic’ anion occupying the position of carbonate. However, an excess of Tiron removes iron from hTF/2N, resulting in an absorption increase at 480 nm and an absorption decrease at 293 nm simultaneously. Experiments showed that a 20-fold excess of Tiron removes iron from hTF/2N almost completely, generating the characteristic spectrum of the apo form.

Spectra were recorded at 5 min intervals after the addition of Tiron for a solution of  $\text{Fe-hTF/2N(CO}_3)$  (Figure 4A). Figure 4B shows the time dependence of the  $A_{480}$ . A pseudo-first-order kinetic equation,  $A = a + b(1 - e^{-kt})$ , where  $a = A_0$ ,  $b = A_\infty - A_0$ , and  $k = k_{\text{obs}}$ , was used to fit the curve and gave a satisfactory result. This simple first-order reaction differs from the biphasic kinetic behavior for the iron release from diferric transferrin by the same ligand, probably because hTF/2N has a single binding site. When the first-order rate constant  $k_{\text{obs}}$  for iron release with different concentrations of Tiron was fitted to the kinetic model (Harris et al., 1992)  $k_{\text{obs}} = k_1[\text{L}]/(1 + k_2[\text{L}])$ , a simple saturation kinetic behavior with respect to the free ligand concentration was found in both the presence and absence of KCl (Figure 5). These saturation kinetics could be interpreted in terms of a rate-limiting conformational change, a basic iron release mechanism proposed in earlier reports (Coward et al., 1982; Chasteen, 1983; Bates, 1982). The retarding effect by chloride ion on the iron release was apparent at all

<sup>2</sup> The absorbance difference at 470 nm for the two forms of hTF/2N complexes,  $\text{Fe-hTF/2N-NTA}$  and  $\text{Fe-hTF/2N-CO}_3$ , was used for the titration under  $\text{CO}_2$ -free conditions. Although these two complexes have close absorption maxima (Bates & Wernicke, 1971), a hyperbolic titration curve was obtained and the saturation point occurred near  $[\text{HCO}_3^-]/[\text{NTA}^{2-}] = 8$ .

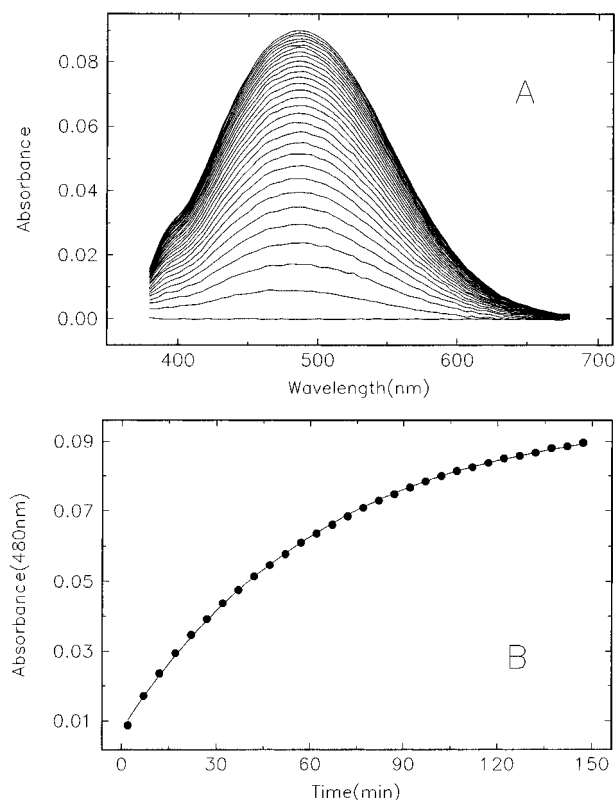


FIGURE 4: (A) Difference spectra for iron release from Fe-hTF/2N(CO<sub>3</sub>) by Tiron (18 mM) in HEPES (50 mM) and KCl (0.5 M), pH 7.4, at 25 °C recorded with 5 min intervals. (B) Dependence of absorbance *vs* time from  $A_{480}$  fitted to a pseudo-first-order kinetic mode.

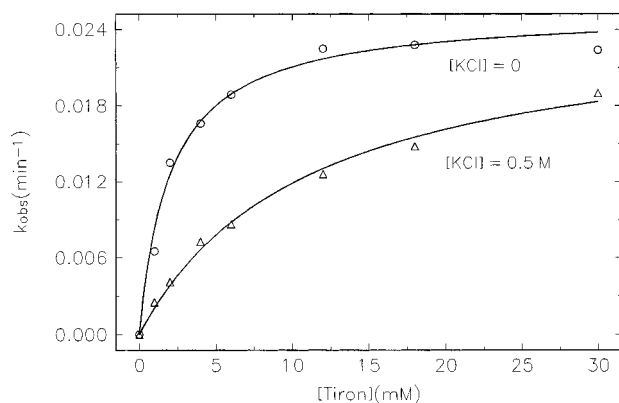


FIGURE 5: Plot of  $k_{\text{obs}}$  for hTF/2N(WT) as a function of increasing concentrations of Tiron in HEPES (50 mM) and KCl (0 and 0.5 M), pH 7.4, at 25 °C.

concentrations of Tiron which were tested. Further experiments were performed to determine in detail the influence of KCl. The results with KCl concentrations up to 2.0 M are shown in Figure 6. Both curves for two different Tiron concentrations display a consistent and interesting trend: the inhibitory effect of chloride has a sharp dependence when  $[\text{KCl}] < 0.5$  M and then levels off after  $[\text{KCl}] > 1.0$  M. With higher Tiron concentration (30 mM), the retarding action of chloride is weaker. Both curves have a minimum  $k_{\text{obs}}$  at around  $[\text{KCl}] = 0.5$  M. This behavior for the retarding effect of chloride may reflect the binding of chloride near the metal-binding site of the protein. Studies on the effect of salt on the EPR spectra of Fe-hTF/2N and several mutants show a similar profile for some plots of the change in EPR amplitude as a function of chloride concentration,

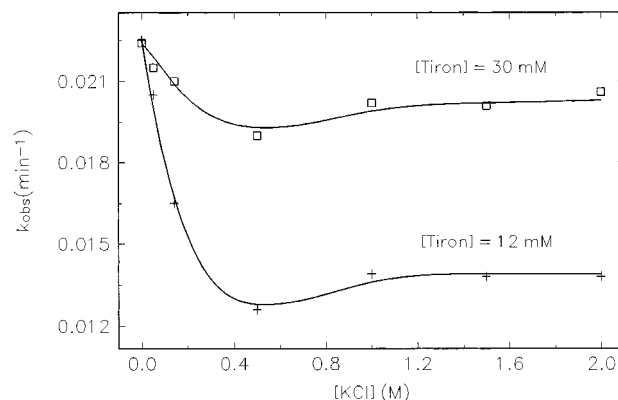


FIGURE 6: Effect of KCl on iron release from hTF/2N(WT) with Tiron (12 and 30 mM) in HEPES (50 mM), pH 7.4, at 25 °C.

with an EPR signal minimum at  $[\text{KCl}] = 0.16$  M (Grady et al., 1995). They interpret the reduction of EPR amplitude to be associated with a conformational change of the protein induced by chloride binding to the transferrin. A more recent study by Harris et al. (1996) showed solid evidence for the binding of chloride to transferrin. In the present case, a competition between chloride and Tiron may exist for binding to a site near the metal center; this could affect iron release from the protein to Tiron. This negative chloride effect is inversely correlated with the concentration of Tiron, supporting the idea of a competition between chloride and the chelator. The minimum  $k_{\text{obs}}$  value at  $[\text{KCl}] = 0.5$  M is assumed to be the saturation point of the chloride binding where the inhibition by chloride reached a maximum. A minor increase of  $k_{\text{obs}}$  after this saturation point may be due to additional effects of high ionic strength on the protein.

Under identical conditions, the reaction between the D63 mutants and Tiron was completed instantly. However, when the solutions after reaction were washed with HEPES buffer (pH 7.4,  $5 \times 2.5$  mL) in a Centricon 10, some orange-violet color still remained even up to a 100-fold excess of Tiron. Spectral measurements showed that these residual solutions have visible absorption bands ( $\lambda_{\text{max}}^{\text{Tiron}}$ , Table 1) at 502, 534, 472, and 483 nm for D63S, D63E, D63N, and D63A, respectively. These absorption maxima in the visible region differ from the  $\lambda_{\text{max}}$ 's for the original proteins and appear to be the characteristic bands for the ternary complexes of iron, Tiron, and the D63 mutants. Interestingly, these  $\lambda_{\text{max}}^{\text{Tiron}}$  values do not follow the order WT > D63E > D63S ~ D63N > D63A, as found in  $\lambda_{\text{max}}$ 's for the normal proteins and the Co(III) complexes; instead, the  $\lambda_{\text{max}}^{\text{Tiron}}$  for wild-type hTF/2N is the lowest, 470 nm. The coordination of Tiron in the D63 mutants thus appears to be quite different from that in wild-type hTF/2N. Perhaps, in hTF/2N, Tiron simply occupies the position of carbonate to provide two ligands to the iron center. This ligation is weak because of the steric strain from the large size of Tiron and does not affect the interaction of Fe-O(Tyr), whereas in the mutants the loss of the Asp 63 may allow accommodation of the large Tiron anion, perhaps by means of a more open conformation, similar to the situation with NTA. This inner flexibility derived from the "loose" interdomain contacts (Faber et al., 1996) may lead Tiron to ligate the iron center intensively (the complex Fe-D63S-Tiron is stable at pH 6.0), which may weaken the interaction between the iron center and the tyrosine ligands so that a large red shift for  $\lambda_{\text{max}}$ 's is observed. Obviously, Tiron is unsuitable as the chelate for kinetic

studies of iron release from the D63 mutants since it can replace, at least partially, carbonate to form complexes with the proteins even when a large excess of Tiron is used. However, it was found that iron release from the D63 mutants could be achieved and monitored using EDTA as the chelating agent. A comprehensive kinetic study for these proteins with EDTA has been conducted, and the results will be presented elsewhere.

In summary, mutations of the metal binding residue Asp 63 in the recombinant N-lobe of human serum transferrin provide a means for investigating the role of this specific residue in the metal-binding properties of the protein. The aspartic acid at position 63 is an essential ligand for tight iron binding in transferrin. The mutations from Asp to Ser, Glu, Asn, and Ala all weakened the ferric ion binding ability considerably, although in all cases binding to metal was observed. Blue shifts of the characteristic absorption bands of the mutants showed the different extent of the effect on the Fe—O(Tyr) interaction. Co(III) exhibited a stronger ligation intensity than Fe(III) in the binding site of the mutants, as demonstrated by significant blue shifts for the characteristic absorption maxima of the Co(III)—mutant complexes. This strong ligation of Co(III) to the mutants was used to determine the extinction coefficients for D63S, D63E, and D63N by means of Co(III) titration. However, the intensive interaction of Co(III) in D63A appeared to result in tyrosine oxidation by Co(III). NTA<sup>2-</sup> displayed a higher affinity than carbonate for binding to the iron center of the mutants, possibly due to the potential of NTA<sup>2-</sup> to act as a tridentate ligand. An intermediate was identified during the conversion from Fe—hTF/2N—NTA to Fe—hTF/2N—CO<sub>3</sub>. Iron release from wild-type hTF/2N by Tiron showed a saturation kinetic behavior with respect to the free ligand concentrations. Chloride has a negative effect on the iron release, which reached a maximum at around [KCl] = 0.5 M, reflecting a saturation of chloride binding to the protein. Iron release experiments for the mutants with Tiron led to the formation of Fe—hTF/2N—Tiron complexes instead of iron removal. This result suggests a different coordination of bound iron with Tiron in all of the mutants when compared to wild-type hTF/2N.

## ACKNOWLEDGMENT

The authors thank Drs. Wesley R. Harris and Kenneth N. Raymond for valuable discussions.

## REFERENCES

- Abdollahi, S., Harris, W. R., & Riehl, J. P. (1996) *J. Phys. Chem.* 100, 1950.
- Anderson, B. F., Baker, H. M., Norris, G. E., Rice, D. W., & Baker, E. N. (1989) *J. Mol. Biol.* 209, 711.
- Bailey, S., Evans, R. W., Garratt, R. C., Gorinsky, B., Hasnain, S. S., Horsburgh, C., Jhoti, H., Lindley, P. F., Mydin, A., Sarra, R., & Watson, J. L. (1988) *Biochemistry* 27, 5804.
- Baker, E. N. (1994) *Adv. Inorg. Chem.* 41, 389.
- Baker, E. N., & Lindley, P. F. (1992) *J. Inorg. Biochem.* 47, 147.
- Baker, E. N., Anderson, B. F., Baker, H. M., Haridas, M., Jameson, G. B., Norris, G. E., Rumball, S. V., & Smith, C. A. (1991) *Int. J. Biol. Macromol.* 13, 123.
- Baldwin, D. A. (1980) *Biochim. Biophys. Acta* 623, 183.
- Bates, G. W. (1982) in *The Biochemistry and Physiology of Iron* (Saltman, P., & Hegenauer, J., Eds.) pp 3–18, Elsevier North-Holland, Inc., Amsterdam.
- Bates, G. W., & Wernicke, J. (1971) *J. Biol. Chem.* 246, 3679.
- Chasteen, N. D. (1983) *Adv. Inorg. Biochem.* 5, 201.
- Chasteen, N. D., & Woodworth, R. C. (1990) in *Iron Transport and Storage* (Ponka, P., Schulman, H. M., & Woodworth, R. C., Eds.) pp 68–79, CRC Press, Boca Raton, FL.
- Cowart, R. E., Kojima, N., & Bates, G. W. (1982) *J. Biol. Chem.* 257, 7560.
- Day, C. L., Anderson, B. F., Tweedie, J. W., & Baker, E. N. (1993) *J. Mol. Biol.* 232, 1084.
- Egan, T. J., Ross, D. C., Purves, L. R., & Adams, P. A. (1992) *Inorg. Chem.* 31, 1994.
- Faber, H. R., Bland, T., Day, C. L., Norris, G. E., Tweedie, J. W., & Baker, E. N. (1996) *J. Mol. Biol.* 256, 352.
- Funk, W. D., MacGillivray, R. T. A., Mason, A. B., Brown, S. A., & Woodworth, R. C. (1990) *Biochemistry* 29, 1654.
- Gaber, B. P., Miskowski, V., & Spiro, T. G. (1974) *J. Am. Chem. Soc.* 96, 6868.
- Grady, J. K., Mason, A. B., Woodworth, R. C., & Chasteen, N. D. (1995) *Biochem. J.* 309, 403.
- Griffiths, E. (1987) in *Iron and Infection* (Bullen, J. J., & Griffiths, E., Eds.) pp 1–25, John Wiley and Sons, Chichester.
- Grossmann, J. G., Mason, A. B., Woodworth, R. C., Neu, M., Lindley, P. F., & Hasnain, S. S. (1993) *J. Mol. Biol.* 231, 554.
- Harris, D. C., & Aisen, P. (1989) in *Iron Carriers and Iron Proteins* (Loehr, T. M., Ed.) pp 239–351, VCH Publishers, Inc., New York.
- Harris, W. R. (1983) *Biochemistry* 22, 3920.
- Harris, W. R. (1986) *Biochemistry* 25, 803.
- Harris, W. R. (1989) *Adv. Exp. Med. Biol.* 249, 67.
- Harris, W. R., & Madsen, L. J. (1988) *Biochemistry* 27, 284.
- Harris, W. R., Bali, P. K., & Crowley, M. M. (1992) *Inorg. Chem.* 31, 2700.
- Harris, W. R., Abdollahi, S., & Cafferty, A. (1996) *Int. Conf. Coord. Chem.*, 31st 92, 5L5 (Abstract).
- He, Q.-Y., Mason, A. B., & Woodworth, R. C. (1996) *Biochem. J.* 318, 145.
- Hsuan, J. J. (1987) *Biochem. J.* 247, 467.
- Kurokawa, H., Mikami, B., & Hirose, M. (1994) *J. Biol. Chem.* 269, 6671.
- Kurokawa, H., Mikami, B., & Hirose, M. (1995) *J. Mol. Biol.* 254, 196.
- Lin, L.-N., Mason, A. B., Woodworth, R. C., & Brandts, J. F. (1993) *Biochem. J.* 293, 517.
- Mason, A. B., Miller, M. K., Funk, W. D., Banfield, D. K., Savage, K. J., Oliver, R. W. A., Green, B. N., MacGillivray, R. T. A., & Woodworth, R. C. (1993) *Biochemistry* 32, 5472.
- MathSoft, Inc. (1996) *Axum Technical Graphics and Data Analysis*, 101 Main St., Cambridge, MA 02142.
- Nelson, R. M., & Long, G. L. (1989) *Anal. Biochem.* 180, 147.
- Nguyen, S. A. K., Craig, A., & Raymond, K. N. (1993) *J. Am. Chem. Soc.* 115, 6758.
- Patch, M. G., & Carrano, C. J. (1981) *Inorg. Chim. Acta* 56, L71.
- Pecoraro, V. L., Harris, W. R., Carrano, C. J., & Raymond, K. N. (1981) *Biochemistry* 20, 7033.
- Rose, T. M., Plowman, G. D., Teplow, D. P., Dreyer, W. J., Hellstrom, K. E., & Brown, T. P. (1986) *Proc. Natl. Acad. Sci. U.S.A.* 83, 1261.
- Ross, D. C., Egan, T. J., & Purves, L. R. (1995) *J. Biol. Chem.* 270, 12404.
- Schlabach, M. R., & Bates, G. W. (1975) *J. Biol. Chem.* 250, 2182.
- Woodworth, R. C., Mason, A. B., Funk, W. D., & MacGillivray, R. T. A. (1991) *Biochemistry* 30, 10824.
- Zak, O., & Aisen, P. (1988) *Biochemistry* 27, 1075.
- Zak, O., Aisen, P., Crowley, J. B., Joannou, C. L., Patel, K. J., Rafiq, M., & Evans, R. W. (1995) *Biochemistry* 34, 14428.

BI963028P